Sugar Transport through Maltoporin of *Escherichia coli*: Role of the Greasy Slide

Patrick Van Gelder,[1,2]† Fabrice Dumas,[1]‡ Ingrid Bartoldus,[3] Nathalie Saint,[2]§ Alexei Prilipov,[2]‖
Mathias Winterhalter,[3]# Yanfei Wang,[2]†† Ansgar Philippsen,[1] Jürg P. Rosenbusch,[2]
and Tilman Schirmer[1]*

*Division of Structural Biology,[1] Division of Microbiology,[2] and Division of Biophysical Chemistry,[3]
Biozentrum, University of Basel, CH-4056 Basel, Switzerland*

The lining of the maltodextrin-specific maltoporin (LamB) channel exhibits a string of aromatic residues, the greasy slide, part of which has been shown previously by crystallography to be involved in substrate binding. To probe the functional role of the greasy slide, alanine scanning mutagenesis has been performed on the six greasy slide residues and Y118 at the channel constriction. The mutants were characterized by an in vivo uptake assay and sugar-induced-current-noise analysis. Crystallographic analysis of the W74A mutant showed no perturbation of the structure. All mutants showed considerably decreased maltose uptake rates in vivo (<10% of the wild-type value), indicating the functional importance of the investigated residues. Substitutions at the channel center revealed appreciably increased (up to 100-fold) in vitro half-saturation concentrations for maltotriose and maltohexaose binding to the channel. Sugar association rates, however, were significantly affected also by the mutations at either end of the slide (W74A, W358A, and F227A), an effect which became most apparent upon nonsymmetrical sugar addition. The kinetic data are discussed on the basis of an asymmetric one-site two-barrier model, which suggests that, at low substrate concentrations, as are found under physiological conditions, only the heights of the extracellular and periplasmic barriers, which are reduced by the presence of the greasy slide, determine the efficiency of this facilitated diffusion channel.

Solute uptake into cells of gram-negative bacteria requires the crossing of two membranes, the outer and the inner membranes, which are separated by the periplasmic space (16). The outer membrane can be considered a defense wall protecting the cell against harmful compounds such as toxins and bile salts. Since a complete seal would impede the import of essential nutrients into the cell, several pore-forming proteins (porins) are located in the outer membrane (19). Transport of solutes through these water-filled channels most commonly proceeds by simple diffusion. For specific porins, diffusional transport is aided by the presence of a binding site.

Maltoporin (LamB) specifically facilitates the translocation of malto-oligosaccharides across the outer membrane barrier. Its crystal structure (20) is trimeric, with each monomer consisting of an 18-stranded β-barrel enclosing a channel. Long loops protrude into the extracellular space, and short turns face the periplasm. Three loops fold into the β-barrel, with loop L3 constricting the channel about halfway through. In the channel lining, there are six contiguous aromatic residues, which form an elongated apolar stripe, the greasy slide, extending from the vestibule through the channel constriction to the periplasmic outlet (Fig. 1). The first of these residues, W74, is provided by L2 of a neighboring subunit. The next three residues, Y41, Y6, and W420, are situated in the middle of the channel. They are followed by W358 and F227, which reside in the wide periplasmic exit hall. A comparable organization of aromatic amino acids has been found in the structures of maltoporin of *Salmonella enterica* serovar Typhimurium (14) and in sucrose-specific channel ScrY (10). Y118 is located opposite to the greasy slide and is the main constituent of the channel constriction about halfway through the channel (Fig. 1).

The structure of maltoporin in complex with maltodextrins (9, 14) shows that the binding site is located at the channel constriction, with the pyranosyl rings of the oligosaccharides engaged in van der Waals contacts with the greasy slide. In addition, the hydroxyl groups of the sugars are H-bonded to an array of predominantly charged protein side chains, dubbed the polar tracks. We have suggested (9, 20) that the end of the greasy slide, which is easily accessible from solvent, helps to thread the sugar into the pore and that subsequent translocation proceeds via one-dimensional diffusion, with the sugar staying in close contact with the slide.

Here, we test this hypothesis by investigating the effect of site-directed mutations of greasy slide residues on in vivo sugar uptake and on the kinetics of maltodextrin binding. Association and dissociation rates were derived from sugar-induced current-noise analysis (2, 15). The role of the residues of the polar tracks has been investigated in a separate study (8).

* Corresponding author. Mailing address: Division of Structural Biology, Biozentrum, University of Basel, Klingelbergstr. 70, CH-4056 Basel, Switzerland. Phone: 41-61-267 20 89. Fax: 41-61-267 21 09. E-mail: tilman.schirmer@unibas.ch.

† Present address: Department of Ultrastructure, VUB, B-1640 Sint-Genesius Rode, Belgium.

‡ Present address: IPBS, CNRS, F-31077 Toulouse, France.

§ Present address: UMR 5048 CNRS 554 INSERM, Centre de Biochimie Structurale, Montpellier, France.

‖ Present address: Ivanovsky Institute of Virology, 123098 Moscow, Russia.

Present address: Institut de Pharmacologie et de Biolgie Structurale, CNRS, University of Toulouse, Toulouse, France.

†† Present address: Department of Biochemistry, Guangzhou Medical College, Guangzhou 510182, People's Republic of China.
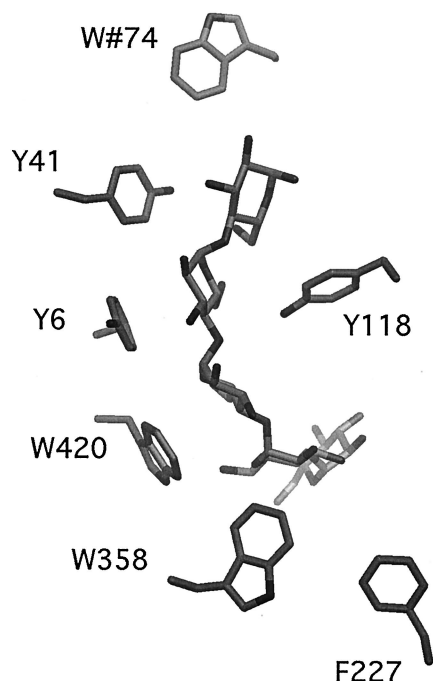
FIG. 1. Side view of the maltoporin channel with maltohexaose (Glc$_6$) bound (9). Only the residues of the greasy slide and residue Y118 at the channel constriction are shown. W74 is part of the extracellular vestibule, whereas W358 and F227 line the periplasmic exit hall. The model was created by graphic program DINO (http://www.dino3d.org).

MATERIALS AND METHODS

Mutagenesis, expression, and purification. Site-directed mutagenesis was performed as described previously (17). Briefly, site-directed mutations were introduced by using single-stranded pBLamB plasmid DNA containing an ampicillin resistance marker in addition to a defect in *ori*, the origin of replication, and the *lamB* gene cloned behind the *phoE* signal sequence under the control of a T7 promoter. Residues of the greasy slide were replaced by alanines, resulting in maltoporin mutants W74A, Y41A, Y6A, W420A, W333A, and F227A. The constricting residue Y118 was equally replaced by an alanine, resulting in mutant protein Y118A. All mutations were confirmed by sequence analysis (Perkin-Elmer ABI; Prism 310 genetic analyzer). DNA manipulations were as described by Sambrook et al. (18).

The mutant maltoporins were expressed in *Escherichia coli* strain BL21(DE3) omp5 (*lamB ompF ompC*) (17), grown in 600 ml of Luria-Bertani medium under selection by ampicillin. Expression was enhanced by addition of 100 μM IPTG (isopropyl-β-D-thiogalactopyranoside). Cells were harvested after overnight growth, and proteins were purified essentially as described previously (17). Prior to sodium dodecyl sulfate-polyacrylamide gel electrophoresis (SDS-PAGE), proteins were incubated for 10 min at room temperature or 100°C in sample buffer; trimers and denatured monomers, respectively, were observed after these treatments (data not shown).

In vivo sugar transport assay. Plasmid transcription was kept at a low level by not including the inducer IPTG in the minimal medium (M9 medium, supplemented with ampicillin [100 μg ml^{-1}] and 0.2% maltose) and relying on "leaky" expression. The bacteria were harvested at late log phase, collected by centrifugation, extensively washed in M9 medium, and resuspended in M9 medium to an optical density at 600 nm of 0.2. Part of the culture was used to prepare cell envelope fractions as described previously (1); the rest was used for the in vivo transport assay. The isolated cell envelopes were analyzed by SDS-PAGE together with a series of increasing amounts of purified LamB of known concentration. After Coomassie blue staining, the protein bands were quantified with a computing densitometer (model 300A; Molecular Dynamics).

Maltose uptake was measured by adding 10 μl of [^{14}C]maltose (ARC Chemical Inc.; specific activity, 600 mCi mmol^{-1}) to 1.5 ml of the cell suspension and adjusting the sugar concentration to 1 μM with nonradioactive maltose. At

different time points after the addition of the sugar, 150 μl of the suspension was filtered through a glass microfiber filter (Whatman GF/C) and cells were washed with 5 ml of M9 medium. The filters were dried for 10 min at 60°C and counted in a scintillation counter.

X-ray structure analysis. Crystallization of the maltoporin mutant W74A was carried out as described before (13). Data from three crystals were collected at 4°C on an Image Plate detector by using an in-house rotating anode as an X-ray source. Processing with programs from the CCP4 suite (3) yielded a data set at 3.5-Å resolution with 83.5% completeness and an overall R_{sym} of 15%; the space group was C222$_1$ ($a = 130.2$ Å, $b = 212.3$ Å, $c = 218.3$ Å). Phases were calculated with difference Fourier methods using the wild-type model (20). Refinement was carried out in XPLOR 3.1 (7) by imposing strict noncrystallographic symmetry constraints, resulting in a model with an R factor of 20.2% (R_{free}, 22.9%) and good stereochemistry.

Fluorescence measurements. Fluorescence emission spectra were measured with a Jasco FP-777 spectrofluorometer. The excitation wavelength was set to 280 nm, and the fluorescence was recorded at 335 nm, with a slit width of 5 nm. Experiments were performed with protein (20 μg/ml) in detergent solution (1% octyl-POE [polyoxyethylene]; Alexis Switzerland). Equilibrium constant $1/K_d^f$ was obtained by plotting $(I - I_o)/I_o$ as a function of the sugar concentration, where I_o and I are the fluorescence intensities in the absence and in the presence of the sugar, respectively. The resulting curve was fitted by using a classical Scatchard plot.

Current-fluctuation analysis. Formation of black lipid bilayers and current-fluctuation analysis were performed as described previously (21). Briefly, maltoporin was reconstituted into black lipid membranes and a potential was applied by a BLM-120 amplifier (Bio-Logic, Claix, France). The ionic current was measured at increasing sugar concentrations. Sugar occupying the binding site leads to a block of the ion current. Release of the sugar molecule restores ion flux through the channels. The frequency of closing events is sugar concentration dependent and is related to the k_{on} rate of sugar binding, while the time the channel is in the closed state reflects the k_{off} rate. The power spectrum of the time course of the ion current was fitted with a Lorentzian, yielding k_{on} and k_{off} rates (11, 15). In symmetric-sugar conditions (sugar added to both compartments), these rate constants reflect access from and release to both sides of the channel. For the determination of individual rates, maltoporin molecules were inserted unidirectionally (80 to 90%) as described previously (21). This was verified by the addition of λ phages (21), which were removed by EDTA treatment before the actual titration of sugar from the *cis* and *trans* sides; the titration was performed to yield the rates over the periplasmic and extracellular entrance barriers, respectively.

RESULTS

Mutagenesis, expression, and structural analysis of maltoporin W74A. The six aromatic residues of the greasy slide and residue Y118 (Fig. 1) of maltoporin from *E. coli* were changed by site-directed mutagenesis one by one to alanine. All proteins were expressed well (results not shown) and were purified. The crystal structure of W74A was determined to 3.5-Å resolution (see Materials and Methods). The difference electron density clearly indicated the absence of the aromatic side chain of the mutated residue, with no other significant changes elsewhere (data not shown). In particular, the conformation of Y41, the adjacent residue on the greasy slide, was found unaltered. Crystallization of other mutant proteins was unsuccessful. The limited success is probably due to the problems with crystallization reproducibility, as it was also observed with the wild-type protein.

In vivo transport of maltose. The influence of the residue replacements on maltose uptake into living cells was determined by using a radiolabeled substrate. Plasmid-encoded maltoporin was expressed at low levels (leaky expression), whereas expression of the other components of the *mal* regulon on the chromosome was fully induced by maltose as the only carbon source. In this way sugar concentrations in the periplasmic space were kept low so that the outer membrane channels were
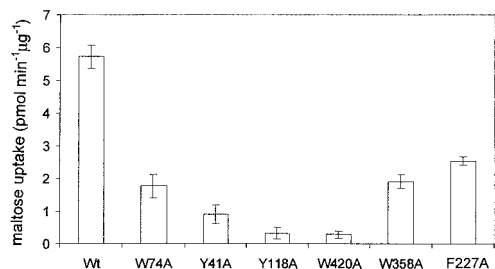
FIG. 2. In vivo uptake rates of [^{14}C]maltose by wild-type maltoporin and alanine mutants. Wt, wild type. The values are means ± standard deviations of four to six independent measurements.

the rate-limiting factor. All mutants showed a decreased maltose uptake rate (6 to 60% of the wild-type rate), revealing the physiological significance of the greasy slide residues and of Y118 in sugar transport (Fig. 2).

Kinetics and thermodynamics of maltodextrin binding. The affinity of maltohexaose (Glc$_6$) for the maltoporin variants was analyzed by monitoring, at various sugar concentrations, the change in protein fluorescence when maltohexaose binds to solubilized proteins. Since aromatic residues constitute a major part of the sugar binding site, a change in the fluorescence signal of aromatic residues was expected and was indeed found (about 10% at saturation). Values of dissociation constant K_d^f derived from the titration experiments are given in Table 1. Replacement of the central residues of the greasy slide (Y41, Y6, and W420) and of Y118 interferes with binding to the greatest degree (increase in K_d^f by more than 100-fold).

The kinetics of maltodextrin binding to maltoporin can be determined by the method of sugar-induced-noise analysis (2, 15). Channels were inserted into a black lipid bilayer immersed in an ionic solution, and an external potential was applied. Since sugar binding blocks ion passage, association and dissociation events are reflected in the time course of the ionic current. Consequently, analysis of the time course at different sugar concentrations can yield the effective kinetic parameters of sugar binding and unbinding, k_{on} and k_{off}, respectively.

For the first series of measurements, Glc$_3$ and Glc$_6$ were added to both sides of the bilayer, and the resulting kinetic data are given in Table 1. These values permit calculation of values of dissociation constant K_d (= k_{off}/k_{on}) for binding of the respective sugars (Table 1). The corresponding changes in

free energy, given by $\Delta G° = -RT\ln (1/K_d)$, where T is the temperature, upon binding to the wild-type channel are −19 and −24 kJ mol^{-1} for Glc$_3$ and Glc$_6$, respectively.

In Fig. 3a, the $\Delta G°$ values for Glc$_6$ binding to the maltoporin variants derived from the kinetic data are compared with the corresponding values deduced from the fluorescence measurements [$\Delta G°_f = -RT\ln (1/K_d^f)$]. It is conspicuous that the $\Delta G°_f$ values for almost all variants are less negative than $\Delta G°$. This can be attributed to the presence of detergent (1% octyl-POE) in the preparations used for the fluorescence measurements. We observed that the detergent lowers the affinity of the sugar for the binding site in a dose-dependent manner (data not shown). In the bilayer experiments, only trace amounts of detergent were present. Apart from this systematic shift, the dissociation constants determined by the two methods agree satisfactorily, supporting the validity of the kinetic measurements. Figure 3b shows values for $\Delta\Delta G°$ (= $\Delta G°_{[mutant]} - \Delta G°_{[wild type]}$), i.e., the change in binding affinity upon the respective mutations. These are discussed below.

It is apparent from Table 1 that, with respect to that for the wild type, the k_{on} rates for the oligosaccharides are reduced in all mutants. The effect is strongest for the mutants that have central residues of the greasy slide replaced (Y41A, Y6A, and W420A) or the opposing residue in the channel truncated (Y118A). This is not surprising, since these residues comprise part of the high-affinity binding site, as has been shown by crystallography (9). But the remaining substitutions at both ends of greasy slide also show significant effects. In the W74 truncation mutant, the Glc$_3$ rate is clearly more affected than the Glc$_6$ rate. It has to be realized that when the sugar is present symmetrically on both sides of the membrane, the measured k_{on} is the sum of the rate constants from both sides of the channel so that the effect of the mutation is actually underestimated. The k_{off} rates are, in general, slightly increased for the mutants with changes at the channel center and significantly reduced for W358A and F227A.

Measuring individual rates requires unidirectional orientation of the channels, which was achieved by application of an external potential during insertion into the bilayer as described before (21). With this approach, 80 to 90% of the channels were oriented with their extracellular sides toward the *trans* compartment, as determined using λ phages that are known to bind to this side of the protein and to block sugar access (21).

TABLE 1. Effects of replacement of aromatic residues at the channel lining by alanine[a]

Maltoporin species	Glc$_3$			Glc$_6$			
	k_{on}, k_1, k_2 (10^6 M^{-1} s^{-1})	k_{off} (10^3 M^{-1})	K_d (mM)	k_{on}, k_1, k_2 (10^6 M^{-1} s^{-1})	k_{off} (10^3 M^{-1})	K_d (mM)	K_d^f (mM)
Wt	8.1 ± 1.9, 7.0 ± 0.1, 3.0 ± 0.1	5.3 ± 0.06	0.65 ± 0.16	17.7 ± 5.0, 18.0 ± 0.8, 5.0 ± 0.1	1.5 ± 0.02	0.085 ± 0.025	0.071 ± 0.015
W74A	2.4 ± 1.3	4.0 ± 0.4	1.7 ± 1.1	11.2 ± 2.4	1.7 ± 0.2	0.15 ± 0.05	1.7 ± 0.56
Y41A	0.8 ± 0.6	5.3 ± 0.8	6.6 ± 6.0	3.6 ± 0.5	3.4 ± 0.1	0.94 ± 0.16	3.3 ± 1.1
Y6A	0.2 ± 0.8	5.4 ± 1.1	27 ± 100	1.0 ± 0.4	3.5 ± 0.2	3.5 ± 1.6	10 ± 10
W420A	1.0 ± 0.4	3.2 ± 0.2	3.2 ± 1.4	0.9 ± 0.3	3.0 ± 0.1	3.3 ± 1.2	5 ± 2.5
Y118A	0.1 ± 0.04	6.0 ± 0.2	60 ± 14	1.3 ± 0.5	3.5 ± 0.3	2.6 ± 1.2	10 ± 6
W358A	3.4 ± 1.3, 3.0 ± 0.2, 0.9 ± 0.1	1.5 ± 0.09	0.44 ± 0.20	8.1 ± 1.5, 7.0 ± 0.2, 0.8 ± 0.1	0.2 ± 0.03	0.025 ± 0.008	0.5 ± 0.13
F227A	4.4 ± 0.8, 3.3 ± 0.1, 1.6 ± 0.1	4.4 ± 0.05	1.0 ± 0.19	11.2 ± 3.3, 9.3 ± 0.4, 1.8 ± 0.3	0.45 ± 0.06	0.040 ± 0.017	0.1 ± 0.004

[a] k_{on} and k_{off} were determined by current-fluctuation analysis with sugar added to both compartments and represent, therefore, apparent rates; the rates have been previously published (11). In addition, for wild-type (Wt) maltoporin and mutants W358A and F227A, "on" rates were measured with vectorially inserted molecules under the asymmetric-sugar condition. The resulting individual "on" rates, k_1 and k_2 (see kinetic scheme in the text), are given. Dissociation constants were obtained from the noise analysis data ($K_d = k_{off}/k_{on}$) and from tryptophan fluorescence quenching (K_d^f). All measurements were repeated at least three times, and the standard deviations are given.
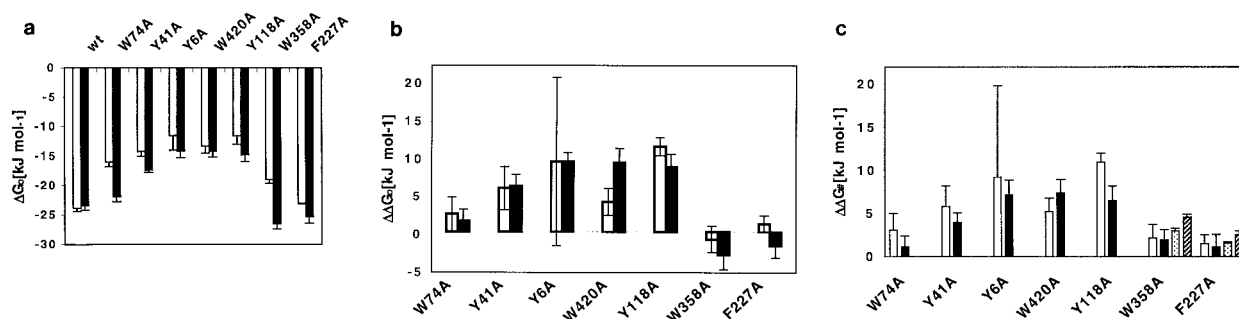
FIG. 3. (a) Change in free energy $\Delta G°$ for Glc_6 binding to wild-type (wt) and mutated maltoporin channels. The results of fluorescence quenching (white bars) and sugar-induced-noise analysis (black bars) are compared. (b) Change in maltoporin binding affinity upon mutagenesis ($\Delta\Delta G° = \Delta G°_{mutant} - \Delta G°_{wild\ type}$) for Glc_3 (white bars) and Glc_6 (black bars). (c) Change in apparent activation energy (symmetric sugar addition) upon mutagenesis ($\Delta\Delta G^{\#} = \Delta G^{\#}_{mutant} - \Delta G^{\#}_{wild\ type}$) for Glc_3 (white bars) and Glc_6 (black bars). For mutants W358A and F227A the changes in the height of the periplasmic barrier (asymmetric sugar addition), $\Delta\Delta G^{\#}_2$, are also given (Glc_3, stippled bars; Glc_6, hatched bars). The values are the means ± standard deviations of at least three independent measurements.

After removal of the phages, sugar was added to the *cis* or *trans* compartment yielding individual "on" rate k_2 or k_1, respectively. These experiments were performed on wild-type maltoporin and on mutants W358A and F227A with results shown in Table 1. Switching from symmetric to asymmetric conditions changed the "off" rates only marginally (data not shown). On the other hand, k_1 and k_2 differ by factors of between 2 and 8 for a given variant (Table 1). Within the limits of error, the sum of the individual rates matches the apparent "on" rate, giving credence to the reliability of the measurements.

DISCUSSION

Maltoporin is the prototype of a guided-diffusion channel. The structure exhibits a binding site in the middle of the channel formed by the central part of the greasy slide and several charged side chains (9, 20). In this study, alanine scanning mutagenesis was employed to study the role of the greasy slide and constriction residue Y118.

The considerable effect of the mutations on sugar import in vivo (Fig. 2) demonstrates the physiological importance of the greasy slide, also suggested by its conservation in distantly related proteins such as sucrose porin ScrY (10). For mutant protein W74A, structural integrity was verified directly by analysis of its crystal structure. For the other mutants, gross structural perturbations of the channel structure can also be ruled out, since, at high concentration, sugar translocation was found almost unaffected in liposome-swelling assays (data not shown). Local structural changes cannot be excluded rigorously, in particular the substitution of those tyrosine residues at the channel center that have their hydroxyl groups bonded to other side chains of the channel lining. It is reassuring, though, that only small changes in the crystal structure of an R100D/Y118D/D121F maltoporin triple mutant were revealed (22).

Considering the minimal structural changes observed in W74A, it is safe to assume that only the entrance barrier is affected by the mutation. In W358A and F227A, at the other end of the slide, the mutated residues are at maximum distance from the extracellular entrance and most probably only the exit barrier will be affected. Therefore, the considerably reduced in vivo uptake rate through these mutant channels gives direct evidence that both ends of the slide, though not part of the

high-affinity binding site (see below), facilitate diffusion of maltose and are of comparable importance (Fig. 2).

The change in free energy ($\Delta G°$) for the transfer of Glc_3 and Glc_6 from solvent to the mutant channels was measured with the variants incorporated in artificial bilayers, thus mimicking the natural environment and avoiding any artifacts due to the presence of detergent in solubilized preparations. The effects of the mutations on the binding affinity, $\Delta\Delta G°$, are virtually the same for Glc_3 and Glc_6 (Fig. 3b). This indicates that, in the wild-type protein, the mutated residues contribute to the binding of the two oligosaccharides in similar ways. In other words, we do not observe a more extended binding site for Glc_6. This is in agreement with the crystal structures of the respective complexes (9), which show that the more extended sugar is curled away from the periphery of the greasy slide. Mutant W420A, however, behaves differently in that $\Delta\Delta G°$ of the Glc_3 complex is less reduced than that of the Glc_6 complex. Truncation of W420 may cause the two saccharides to bind in different modes. It is conceivable that, for example, the short sugar can adopt a favorable binding position on the greasy slide adjacent to the mutated residue. Glc_6, on the other hand, would have to span the mutated site or bind also to the periphery; in both cases its binding capacity would not fully be satisfied. It is noteworthy that for the maltoporin Y118F mutation also a significant sugar length dependence of the binding affinity (normalized to the wild-type values) has been observed (4). This may reflect a similar situation.

While $\Delta\Delta G°$ is small for the W74 truncation mutant (as described previously for the more drastic W74R mutation [4]) and is virtually zero for the mutations at the periplasmic end of the slide (W358 and F227), a considerable difference for the other mutants is observed. The large decrease in binding affinity upon truncation of Y41, Y6, and W420 emphasizes their role in the interaction with the pyranose rings (Fig. 1). Intriguingly, truncation of Y118, which faces the center of the greasy slide across the channel constriction, exhibits a similar effect. Since this residue contributes to the shape complementary of the channel with respect to maltodextrins, it is probably important for proper alignment of the sugar with the binding site. The inverse effect (stabilization of the complex) was reported for the Y118F maltoporin mutant (12), probably due to the increased hydrophobicity of the channel constriction and con-

comitant enhancement of the hydrophobic interaction with the sugar.

The main goal of the current-induced-noise analysis was to get a more detailed insight into the kinetics of sugar binding and into the role of the residues at the two ends of the slide that appear not to be part of the sugar binding site. A simple one-side, two-barrier kinetic model has been proposed previously (5, 12) to describe the maltodextrin-maltoporin complex formation (S_{extrac}, sugar at the extracellular side; P, protein [i.e., the maltoporin channel]; S_{perip}, sugar at the periplasmic side)

$$S_{extrac} + P \underset{k_{-1}}{\overset{k_1}{\rightleftharpoons}} S\,P \underset{k_{-2}}{\overset{k_2}{\rightleftharpoons}} S_{perip} + P$$
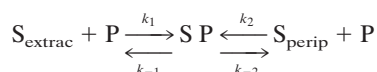
In the proposed symmetric model the heights of the two access barriers and, hence, the individual "on" and "off" rates were assumed to be equal. For the interpretation of our results, we have to abandon this simplification, since some of the mutations are expected, by design, to affect only one or the other of the barriers. Furthermore, it has been shown recently that even for wild-type maltoporin the two "on" rates differ (21) (see below). In an asymmetric model and with substrate present only on the extracellular side, the flux through the channel is given by

$$\Phi = k_1[1 - 1/(1 + k_{-2}/k_{-1})]c \qquad (1)$$

if substrate concentrations are small ($k_1 c \ll [k_{-1} + k_{-2}]$) and by

$$\Phi_{max} = k_{-2} \qquad (2)$$

if concentrations are saturating (generalization of the formalism in reference 12). Maltoporin catalyzes the flux of maltodextrin across the outer membrane at low external substrate concentrations (for a detailed discussion see reference 6), the situation modeled by equation 1. Under this condition, three rate constants seemingly determine the flux. However, since k_{-2}/k_{-1} is independent of the depth of the energy well, it turns out that the flux is exclusively determined by the heights of the two barriers. The presence of a binding site, though, is probably important to compensate for the loss of sugar hydration and may in fact lower the barrier heights. From the apparent "on" rates, the height of the effective activation energy for sugar binding, $\Delta G^{\#}$ ($= -RT\ln k_{on} + RT\ln k_o$), with k_o being the substrate-to-channel collision rate, can be calculated. This can be compared to the wild-type activation energy, yielding $\Delta\Delta G^{\#} = \Delta G^{\#}_{mutant} - \Delta G^{\#}_{wild\ type}$, the change in activation barrier height caused by the mutation displayed in Fig. 3c. First, note that the profiles for Glc_3 and Glc_6 superimpose rather well, which indicates that the investigated residues play similar roles in the association process. An exception may be W74, which appears to be more important for the "on" process of Glc_3 than for that of Glc_6.

Because the sugar was added to both sides of the membrane, the observed "on" rates reflect movement of the substrate through both entryways and the effect of a mutation at one of the entrances is underestimated. Probing the two entryways individually (Table 1) reveals that k_1 is smaller than k_2 by a factor of 2 to 3 in the wild type. This is in good agreement with

previous titration experiments (21). An unchanged "on" rate over the extracellular barrier would be expected following replacement of W358 and F227 at the periplasmic end of the slide; instead a significant decrease in the k_1 values (about 50%) was found. The reason for this is unclear, since it can be ascribed only partly to the fraction of oppositely oriented channels. The k_2 values are, however, in general much more affected (Table 1), and the corresponding $\Delta\Delta G^{\#}_2$ values are displayed in Fig. 3c. The data suggest that the mutations have a more pronounced effect on the height of the activation barrier for the longer Glc_6. In this context it is noteworthy that the homologous sucrose-specific ScrY porin lacks an aromatic equivalent of F227. Clearly, probing the barriers individually is the method of choice and should be applied to the other mutants.

To conclude, we have shown that in the framework of a simple kinetic model the efficiency of the maltoporin channel is determined, at a physiological sugar concentration, by the heights of the two activation barriers. Site-directed mutagenesis and functional analysis revealed that these barriers are lowered by the greasy slide that extends at either side into the two channel vestibules. There, the slide helps to align the sugar with the channel axis and facilitates, in concert with the polar tracks (8), the sugar hydration/dehydration process.

REFERENCES

1. **Agterberg, M., H. Adriaanse, H. Lankhof, R. Meloen, and J. Tommassen.** 1990. Outer membrane PhoE protein of Escherichia coli as a carrier for foreign antigenic determinants: immunogenicity of epitopes of foot-and-mouth disease virus. Vaccine **8:**85–91.
2. **Andersen, C., M. Jordy, and R. Benz.** 1995. Evaluation of the rate constants of sugar transport through maltoporin (LamB) of E. coli from the sugar-induced current noise. J. Gen. Physiol. **105:**385–401.
3. **Anonymous.** 1994. Collaborative computational project, number 4. The CCP4 suite: programs for protein crystallography. Acta Crystallogr. **D50:**760–763.
4. **Benz, R., G. Francis, T. Nakae, and T. Ferenci.** 1992. Investigation of the selectivity of maltoporin channels using mutant LamB proteins: mutations changing the maltodextrin binding site. Biochim. Biophys. Acta **1104:**299–307.
5. **Benz, R., A. Schmid, and G. H. Vos-Scheperkeuter.** 1987. Mechanism of sugar transport through the sugar-specific LamB channel of Escherichia coli outer membrane. J. Membr. Biol. **100:**21–29.
6. **Boos, W., and H. Shuman.** 1998. Maltose/maltodextrin system of Escherichia coli: transport, metabolism, and regulation. Microbiol. Mol. Biol. Rev. **62:**204–229.
7. **Brünger, A. T.** 1992. X-PLOR manual, version 3.1. Yale University, New Haven, Conn.
8. **Dumas, F., R. Koebnik, M. Winterhalter, and P. Van Gelder.** 2000. Sugar transport through maltoporin of Escherichia coli. Role of polar tracks. J. Biol. Chem. **275:**19747–19751.
9. **Dutzler, R., Y.-F. Wang, P. J. Rizkallah, J. P. Rosenbusch, and T. Schirmer.** 1996. Crystal structures of various maltooligosaccharides bound to maltoporin reveal a specific sugar translocation pathway. Structure **4:**127–134.
10. **Forst, D., W. Welte, T. Wacker, and K. Diederichs.** 1998. Structure of the sucrose-specific porin ScrY from Salmonella typhimurium and its complex with sucrose. Nat. Struct. Biol. **5:**37–46.
11. **Hilty, C., and M. Winterhalter.** 2001. Facilitated substrate transport through membrane proteins. Phys. Rev. Lett. **86:**5624–5627.
12. **Jordy, M., C. Andersen, K. Schulein, T. Ferenci, and R. Benz.** 1996. Rate constants of sugar transport through two LamB mutants of Escherichia coli: comparison with wild-type maltoporin and LamB of Salmonella typhimurium. J. Mol. Biol. **259:**666–678.
13. **Keller, T. A., T. Ferenci, A. Prilipov, and J. P. Rosenbusch.** 1994. Crystallization of monodisperse maltoporin from wild-type and mutant strains of various Enterobacteriaceae. Biochem. Biophys. Res. Commun. **199:**767–771.

14. **Meyer, J. E. W., M. Hofnung, and G. E. Schulz.** 1997. Structure of malto-porin from Salmonella typhimurium ligated with a nitrophenyl-maltotrioside J. Mol. Biol. **266:**761–775.

15. **Nekolla, S., C. Andersen, and R. Benz.** 1994. Noise analysis of ion current through the open and the sugar-induced closed state of the LamB channel of *E. coli* outer membrane: evaluation of the sugar binding kinetics to the channel interior. Biophys. J. **66:**1388–1397.

16. **Nikaido, H., and M. Vaara.** 1985. Molecular basis of bacterial outer membrane permeability. Microbiol. Rev. **49:**1–32.

17. **Prilipov, A., P. S. Phale, P. Van Gelder, J. P. Rosenbusch, and R. Koebnik.** 1998. Coupling site-directed mutagenesis with high-level expression: large scale production of mutant porins from E. coli. FEMS Microbiol. Lett. **163:**65–72.

18. **Sambrook, J., E. F. Fritsch, and T. Maniatis.** 1989. Molecular cloning: a laboratory manual, 2nd ed. Cold Spring Harbor Laboratory Press, Cold Spring Harbor, N.Y.

19. **Schirmer, T.** 1998. General and specific porins from bacterial outer membranes. J. Struct. Biol. **121:**101–109.

20. **Schirmer, T., T. A. Keller, Y.-F. Wang, and J. P. Rosenbusch.** 1995. Structural basis for sugar translocation through maltoporin channels at 3.1 Å resolution. Science **267:**512–514.

21. **Van Gelder, P., F. Dumas, J. P. Rosenbusch, and M. Winterhalter.** 2000. Oriented channels reveal asymmetric energy barriers for sugar translocation through maltoporin of Escherichia coli. Eur. J. Biochem. **267:**79–84.

22. **Van Gelder, P., R. Dutzler, F. Dumas, R. Koebnik, and, T. Schirmer.** 2001. Sucrose transport through maltoporin mutants of Escherichia coli. Protein Eng. **14:**943–948.